AAS 19-108

TESTING OF THE LUNAR RECONNAISSANCE ORBITER ATTITUDE CONTROL SYSTEM RE-DESIGN WITHOUT A GYRO

Julie Halverson (formerly Thienel),[*]
Phil Calhoun, Oscar Hsu, and Jean-Etienne Dongmo,[†]
Rebecca Besser, Ben Ellis, Russell DeHart, Yohannes Tedla,[‡]
Sean Rosney,[§] Scott Snell,[¶]

The Lunar Reconnaissance Orbiter (LRO) was launched in 2009 and, with its seven science instruments, has made numerous contributions to our understanding of the moon. LRO is in an elliptical, polar lunar orbit and nominally maintains a nadir orientation. There are frequent slews off nadir to observe various science targets. LRO attitude control system (ACS) has two star trackers and a gyro for attitude estimation in an extended Kalman filter (EKF) and four reaction wheels used in a proportional-integral-derivative (PID) controller. LRO is equipped with thrusters for orbit adjustments and momentum management. In early 2018, the gyro was powered off following a fairly rapid decline in the laser intensity on the X axis. Without the gyro, the EKF has been disabled. Attitude is provided by a single star tracker and a coarse rate estimate is computed by a back differencing of the star tracker quaternions. Slews have also been disabled. A new rate estimation approach makes use of a complementary filter, combining the quaternion differentiated rates and the integrated PID limited control torque (with reaction wheel drag and feedforward torque removed). The filtered rate estimate replaces the MIMU rate in the EKF, resulting in minimal flight software changes. The paper will cover the preparation and testing of the new gyroless algorithm, both in ground simulations and inflight.

INTRODUCTION

The Lunar Reconnaissance Orbiter (LRO) was launched on June 18, 2009. The original mission focus was on supporting the extension of human presence in the solar system. After the Exploration Mission phase completed in 2010, LRO became a part of NASA's Science Mission Directorate and began its Science Mission. Throughout the mission life LRO has collected a vast quantity of data, greatly increasing our knowledge about the moon. LRO is equipped with the following seven instruments: Cosmic Ray Telescope for the Effects of Radiation (CRaTER), Diviner Lunar Radiometer (DLRE), Lyman Alpha Mapping Project (LAMP), Lunar Exploration Neutron Detecter (LEND), Lunar Orbiter Laser Altimeter (LOLA), Lunar Reconnaissance Orbiter Camera (LROC), and the mini-RF technology demonstration. Figure 1 is an image of the Apollo 11 landing site taken by LROC.[1]

[*]Space Sciences Mission Operations, NASA/GSFC, Greenbelt, MD 20771.
[†]Guidance, Navigation, and Control, NASA/GSFC, Greenbelt, MD 20771.
[‡]KBRwyle, Greenbelt, MD 20771.
[§]ASRC Federal Technical Services, Greenbelt, MD 20771
[¶]Northrup Grumman Corporation, Greenbelt, MD 20771.

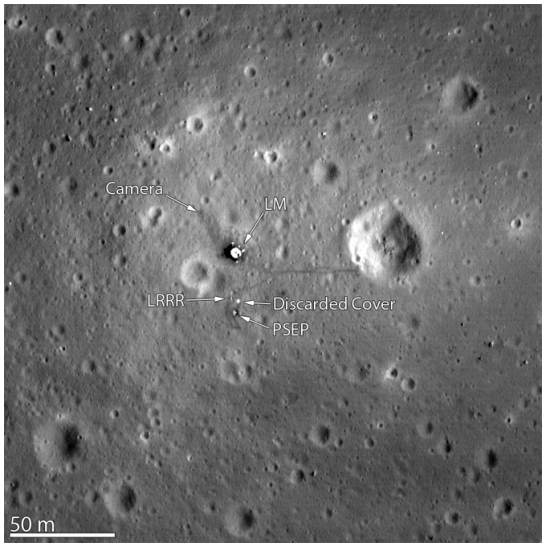

Figure 1. Apollo 11 Landing Site (Courtesy of NASA Goddard/Arizona State University)

Figure 2 is an image of the LRO spacecraft. LRO has ten coarse sun sensors, two star trackers, and a miniature inertial measurement unit (MIMU). An extended Kalman filter (EKF) estimates the spacecraft attitude using the star tracker quaternions and the MIMU data. The attitude control system has four modes of operation: Observing, Momentum Management, Orbit Maintenance, and Sun Safe. The Attitude Control System (ACS) is three-axis stabilized, and the Observing mode provides nadir, off-nadir, and inertial fine pointing in support of science observations, instrument calibrations, and special imaging. LRO has a set of four reaction wheels and a reaction control system for momentum unloading.[2] The LRO orbit is an approximately 30 km by 200 km altitude elliptical orbit with an inclination of approximately 86 deg and orbital period of 2 hours. During the course of a year the beta angle goes through a full cycle from -90 deg to +90 deg and back to -90 deg, passing through 0 deg twice. At beta angles (absolute value) of less than 37.5 degrees, the solar array tracks the sun. Otherwise it remains parked. The changing beta angle causes temperature fluctuations in numerous spacecraft components; in particular at low beta angles the star tracker optics and CCD temperatures are highest. The star tracker temperature fluctuations affect the star tracker alignment and they also affect the quality of the star tracker quaternion and the speed at which the star tracker recovers following an occultation or unexplained reset. The star tracker alignments were recently estimated and updated onboard, and the star tracker thermal electric cooler set point was lowered. Both activities should result in improved star tracker performance during gyro-less operations.

In late 2017, the MIMU laser intensity monitor current on the X axis began declining. In March 2018, with about 625 hours of estimated life remaining in the X axis, the MIMU was powered off. The EKF was disabled and all slews were suspended. Initially the MIMU was powered on for off-axis momentum unload maneuvers, but those have since been replaced with in-line gyroless 'one-shot' momentum unloads. The MIMU was powered on during a long eclipse in July 2018 and again during a January 2019 eclipse. If a fault occurs on the spacecraft, the MIMU will be powered on and the spacecraft will slew to a sun-pointing orientation. In nominal operations with the MIMU off, the angular velocity is estimated by differentiating the star tracker quaternions and the attitude is provided from a single star tracker. The rate estimates are noisy and dependent on the quality

Figure 2. Lunar Reconnaissance Orbiter (Courtesy of NASA/LRO)

and availability of the star tracker data. When a star tracker is predicted to be occulted, the flight operations team must send a command to the spacecraft to remove that star tracker from the rate estimation and ensure it is not selected as the source of the attitude.

In 2014, a preliminary study indicated that applying a complementary filter to the star tracker differentiated quaternions and the commanded wheel torque could result in a rate estimate to replace the MIMU in the EKF.[3] A high-fidelity (HiFi) simulation was developed for LRO for prelaunch testing and validation of the ACS algorithms. In addition, LRO maintains a software-based simulator and a hardware-based FlatSat to test operational procedures prior to uplink to the spacecraft. The paper will cover the preparation and testing of the new complementary filter rate-based EKF in the HiFi, the development of the new FSW code, the results of simulator testing, and finally the initial inflight results following a successful upload of the software to the spacecraft.

COMPLEMENTARY FILTER

The quaternion kinematics, given in equation 1, and Euler's equation, given in equation 2, are both a function of the angular velocity.

$$\dot{q} = \frac{1}{2} Q(q)\omega \tag{1}$$

$$T = \frac{d}{dt}(I\omega + h) + \omega \times (I\omega + h) \tag{2}$$

where q is the quaternion, $Q(q)$ is a 4×3 matrix, ω is the angular velocity, T is torque, I is the spacecraft inertia, and h is the reaction wheel angular momentum.

The Observing mode attitude controller is a quaternion-feedback, PID controller designed to produce reaction wheel torque commands. The estimated gyroscopic torque is added to the PID control torque which is then filtered, transformed into the reaction wheel frame, and adjusted for reaction wheel drag. The final wheel torque commands are limited and then redistributed to the wheels with the Mini-Max wheel momentum redistribution.[4] Without the MIMU, an alternative method for rate estimation is necessary. One option is to redesign the EKF to estimate attitude and rate, a significant flight software change. The other alternative is to estimate the rate outside the EKF and use the estimate as a replacement to the MIMU-provided rate. A complementary filter is

a method of combining two different measurement sources to estimate a single variable, when the two measurements have different frequency characteristics.[5] The first measurement is derived from equation 1.

$$\hat{\omega}_{ST} = 2Q(q_{ST})^T \dot{q}_{\text{ST}} \tag{3}$$

where q_{ST} indicates the quaternion from a star tracker (ST). The second measurement, given in Equation 4, is obtained by integrating the angular acceleration calculated from the spacecraft inertia (inverse) and the PID controller estimated wheel torque.

$$\dot{\hat{\omega}}_{RW} = I^{-1}(-T_{\text{m}} - T_{\text{ffwd}}) \tag{4}$$

where T_{m} is the commanded wheel torque, with the drag compensation and gyroscopic torque (T_{ffwd}) removed. The complementary filter applied to LRO minimizes the low frequency noise from the quaternion differentiation and the high frequency noise from the controller estimated torque. Equation 5 is a conceptual expression of the complementary filter in the frequency domain.

$$\hat{\omega}(s) \approx \frac{\omega}{s+\omega}\left[(2Q^T sq(s)\right] + \frac{s}{s+\omega}\left[\frac{1}{s}(I^{-1}T)\right] \tag{5}$$

The complementary filter is implemented inflight using an existing second-order discrete filter. The second-order filter is used by the controller as a structural filter to suppress low frequency spacecraft modes, with filter coefficients provided through a flight software table.[2] This same filter is used as a high pass filter for the star tracker rate terms and a low pass filter for the reaction wheel integrated rate term.

Using the LRO bandwidth of approximately 0.05Hz and the ACS sample time of 0.2 sec, the coefficients for each filter were determined through the use of MATLAB's continuous to discrete transformation function. Figure 3 shows that the low frequency components from the quaternion differentiation and high frequency components from the angular acceleration integration are eliminated. The figures show good agreement between the continuous (black line) and discrete responses (blue line).

EKF OVERVIEW AND ALGORITHM UPDATES

The EKF filter traces its history to an algorithm proposed by Murrell in 1978.[6] Several NASA missions used independent modules designed for replacement and were known as Multimission Modular Spacecraft (MMS). The first such mission was the Solar Maximum Mission (SMM).[7] Murrell proposed a Kalman filter design for the attitude determination in the MMS that utilized scalar updates, avoiding matrix inversion and reducing the computational load. Several NASA missions after SMM made use of this onboard filter, including the Tropical Rainforest Measuring Mission (TRMM) and the Wilkinson Microwave Anisotropy Probe (WMAP). The LRO EKF is based heavily on the TRMM and WMAP filters.

The EKF is implemented as a discrete Kalman filter following the standard equations for covariance propagation and state and covariance update.[8]

$$P_k(-) = \Phi_{k-1} P_{k-1} \Phi_{k-1}^T + Q_{k-1} \tag{6}$$

$$K_k(-) = P_k H_k^T [H_k P_k H_k^T + R]^{-1} \tag{7}$$

$$\underline{\hat{x}}_k(+) = \underline{\hat{x}}_k(-) + K_k[\underline{z}_k - H_k \underline{\hat{x}}_k(-)] \tag{8}$$

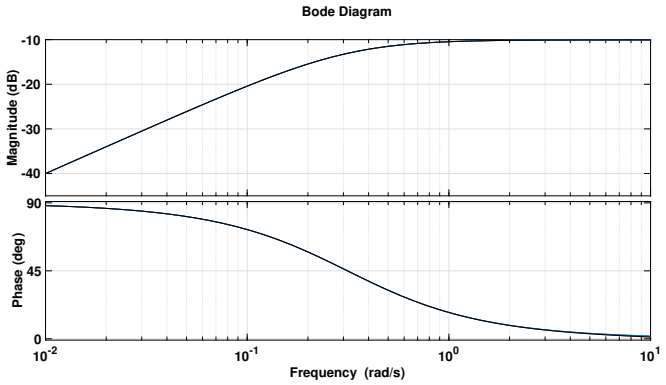

(a) Star Tracker Quaternion Differentiation

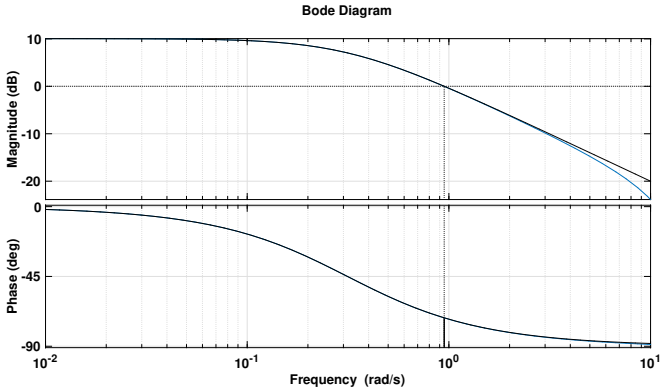

(b) Angular Acceleration Integration

Figure 3. Bode Plots for Complementary Filter Measurements

$$P_k(+) = [I - K_k H_k] P_k(-) \tag{9}$$

Where P is the covariance matrix of the error states, Q is the process noise covariance matrix, Φ is the state transition matrix, K is the Kalman gain, H is the measurement matrix, R is the measurement noise covariance matrix, $\underline{z}$ is the effective measurement, and $\underline{x}$ is the error state vector. The $\hat{}$ refers to an estimated quantity, $(+)$ refers to a posteriori estimates and $(-)$ refers to a priori estimates.

The gyro-based EKF state consists of the attitude quaternion and gyro bias. The attitude quaternion is propagated according to equation 3 and the bias is modeled as a random walk.

$$\dot{\underline{b}} = \underline{\eta}_u \tag{10}$$

The gyro model is given as

$$\underline{\omega}_g = \underline{\omega} + \underline{b} + \underline{\eta}_v \tag{11}$$

The terms $\underline{\eta}_u$ and $\underline{\eta}_v$ are Gaussian distributed white noise vectors with zero mean and standard deviations given by $\underline{\sigma}_u$ and $\underline{\sigma}_v$, respectively. In the gyroless EKF, the gyro data, $\underline{\omega}_g$, is replaced with the rate estimate from the complementary filter

$$\hat{\underline{\omega}}_g = \frac{1}{n}\left(\sum_{i=1}^{n} \hat{\underline{\omega}}_{ST,i}\right) + \hat{\underline{\omega}}_{RW} \tag{12}$$

where n can be either 1 or 2, depending on the number of star tracker quaternions available. If a star tracker is occulted, n is 1 and the rate is estimated with a single star tracker and the reaction wheel control term. If the occulted star tracker becomes available, n is 2 and the star tracker rate estimates are averaged and added to the reaction wheel control term. The rest of the EKF algorithm is unchanged. The state is updated with the measurements from the star trackers. The star tracker quaternions are transformed into the body frame and then used to generate a measurement of the attitude error. The attitude error is the vector part of the delta quaternion formed as the multiplicative difference between the measured star tracker quaternion and the current EKF quaternion estimate. The details of the EKF update are provided in [8].

TEST ENVIRONMENT

High-Fidelity Simulation

During the LRO development, a comprehensive dynamic simulation was developed for GNC testing. The HiFi simulation is implemented in Matlab's Simulink environment. Prior to implementing the complementary filter and updating the rate input to the EKF, the HiFi was upgraded to better match the current state of the spacecraft. The inertia and mass were updated to reflect nine years of fuel depletion from momentum unloads and orbit maintenance. The reaction wheel and star tracker truth model noise parameters were also updated to reflect noise observed in actual flight data. In addition, the HiFi was enhanced to allow initialization with real data, to read spacecraft ephemerides, and to conduct slews using the same commanding as onboard. Data produced from the HiFi was compared to real spacecraft data for fifty-two cases throughout 2016. The test cases covered both yaw orientations (LRO rotates 180 deg twice per year based on the beta angle), a full range of beta angles and a comprehensive set of science slews. Additionally both tracking and parked solar array configurations were evaluated, including a simulated spacecraft response to the stopping, starting, and accelerating of the solar array gimbal. The tests were conducted with the gyro-based EKF and with the differentiated quaternion rate estimate that has been used onboard since the gyro was powered off. Figure 4 is an example comparing the onboard, HiFi estimated, and truth model system momentum components over a day. The data includes a multi-axis slew and several pitch slews. The values all agree well, generally within a few Newton-meter-seconds (Nms). Figure 5 is an example comparing the HiFi gyro data (blue), and the onboard gyro data (red), again with several slews included.

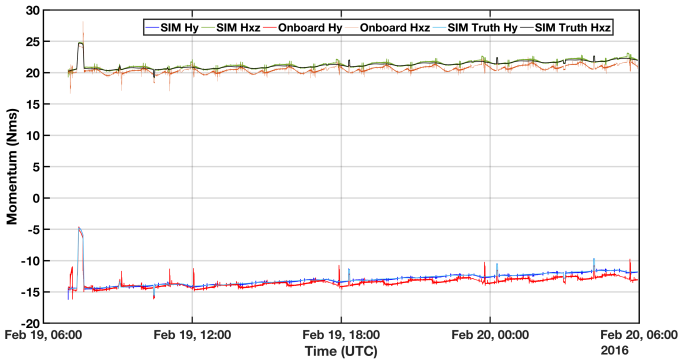

Figure 4. HiFi Momentum Comparison to Onboard and Truth

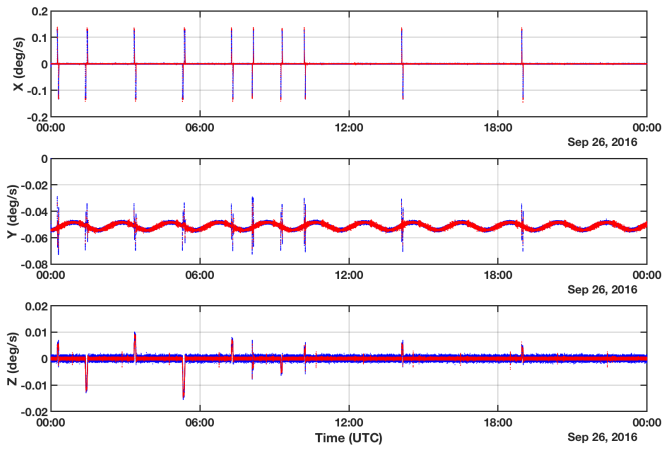

Figure 5. HiFi Gyro Data Comparison to Onboard, with Several Slews Included

Once the HiFi was validated against real flight data, the complementary filter components were incorporated along with changes necessary to use the estimated rate in place of the gyro. A star tracker derived rate using equation 3 exists in the flight software. A reaction wheel torque derived rate estimate was also included during development but never used. It was modified according to equation 4 and included along with the second-order filter coefficients. The complementary filtered rate is corrected for a bias estimated by the EKF. New EKF tuning parameters proposed in Reference 3 were used in testing. The process noise terms, σ_u and σ_v, the a priori covariance, and the star tracker measurement noise uncertainty were all increased. Additionally the covariance convergence and divergence thresholds were both also increased. Otherwise the EKF itself remains unchanged.

As described previously, the complementary filter is implemented within an existing onboard second-order filter with the coefficients determined as described above. When a star tracker becomes occulted, the quaternion output from the star tracker processing becomes stale and the data is marked as invalid. In order to prevent large errors in the derived rates by using old measurements, the star tracker filter is reset every time a measurement is invalid. Additionally, a wait time is introduced following a reset, to allow the filter to settle. The reaction wheel torque filter is also reset if it is disabled for any reason. (For example, if the gyro is powered on for an orbit maneuver the complementary filter terms will be disabled.) In addition, the EKF residual editing is disabled. If the star trackers are ever inadvertently occulted simultaneously the filter covariance increases and the attitude and rate errors grow. When a star tracker then becomes unocculted, the residuals could be large. But, if the measurements are accepted by the EKF, the filter converges quickly.

LRO Simulators

There are two flight simulators maintained for LRO, a software-based simulation and a hardware-based simulation.[9] The software-based simulator is an engineering test unit of the LRO command and data handling unit (CDH). The simulator connects to a dynamic truth model and contains a complete copy of the LRO flight software. The CDH simulator can be used to test new code, table updates, commands, and procedures. Spacecraft telemetry is produced and is used to evaluate the performance of the test. The hardware-based simulator, known as FlatSat, was developed for

spacecraft integration and testing, and was built with hardware engineering test units. FlatSat also connects to a dynamic truth model and, like the CDH simulator, produces spacecraft telemetry for evaluation. FlatSat is also used for procedure testing,hardware and software testing, system level flight software testing, and personnel training.

After the completion of the HiFi testing, the complementary filter and updates to the Kalman filter were documented in an LRO attitude control system algorithm description document. The algorithm document serves as the basis for the flight software updates. Flight software development follows a rigorous process of review and testing before uplink to the spacecraft. The process includes the following phases: requirements analysis, software design, implementation, and test. After each phase a review is held and all open actions are addressed before proceeding to the next phase. The flight software was modified to include the complementary filter and was tested on both the CDH simulator and the FlatSat simulator. Several test scenarios were developed to test loading of the new patch, transitioning between modes on the spacecraft, star tracker occultations, slewing, and fault detection. New telemetry points were created and additional parameters were added to tables.

RESULTS

HiFi Test Results

Monte Carlo testing was conducted with the new angular rate measurements in the EKF, comparing the results to the truth model in the HiFi. Scenarios were selected to cover a range of beta angles and varying initial angular momentum. Noise terms and misalignments were varied for the star tracker and reaction wheels, along with the initial attitude. Tests were run with and without slews that encompassed representative science targets from small slew angles to large multi-axis slews. Figure 6 shows the knowledge errors and pointing errors from six different days that were selected from 2016; each day includes 500 Monte Carlo runs, each four hours in length (two orbits). The blue line in each plot is the original requirement for both knowledge and overall pointing error, ± 30 arcsec (3σ) and ± 45 arcsec (3σ), respectively. In all the Monte Carlo cases run, the EKF performed well and the controller remained stable. The only scenario that caused large errors was simultaneously occulting both star trackers. Figure 7 is an example of the attitude errors growing during a slew that resulted in a prolonged simultaneous occultation. In this case both star trackers are invalid due to the occultations and, had this happened inflight, the spacecraft would transition to the sun safe mode. The operational slew planning tools have been modified to check for simultaneous occultations, and if discovered will prevent such slews from being uploaded to the spacecraft. In addition, the star tracker residual edit tests have been disabled, to allow any star tracker measurement declared valid to be used by the EKF.

FlatSat Testing

Several scenarios were prepared to test the performance of the LRO flight software in both the CDH simulator and in FlatSat, including a test of the installation of the flight software patch. For the installation test the MIMU was powered on, the spacecraft was placed into the sun safe mode, and all the instruments were powered off. The patch was uploaded and installed. The spacecraft was returned to nadir pointing, the rate source was switched to the complementary filter rate estimate, the EKF was successfully enabled, and the MIMU was powered off. Other cases tested science slews, momentum unloads, and an extended eclipse. All cases used actual inflight scenarios run with the complementary EKF rather than the gyro-based EKF or the quaternion differentiated rate. Figure 8 contains example results showing the controller rate errors. The scenario in Figure 8 includes a 90

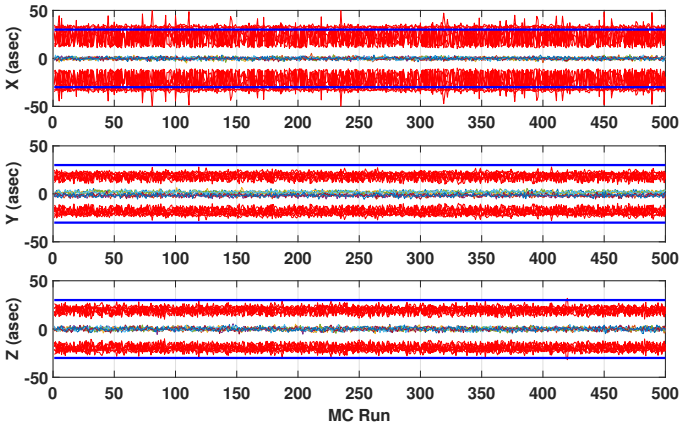

(a) Mean Knowledge Errors with $\pm 3\sigma$ (Red) and Knowledge Requirement (Blue)

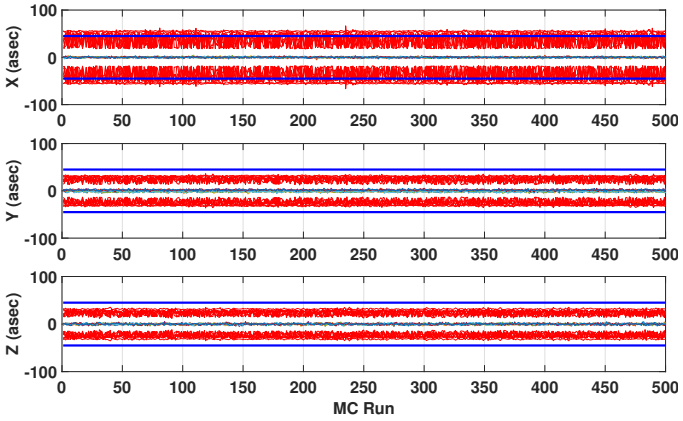

(b) Mean Pointing Errors with $\pm 3\sigma$ (Red) and Pointing Requirement (Blue)

Figure 6. Monte Carlo Test Results

deg yaw slew, a 180 deg yaw slew, and a stationkeeping maneuver. The controller remained stable and successfully performed all slews.

Inflight Results

The FSW patch was successfully loaded, installed, and activated on the spacecraft on December 12, 2018. The installation steps were identical to those conducted in the FlatSat test installation with a slew to the sun safe mode for the installation. Upon returning to nadir pointing after the installation, the complementary filter rate was selected as the rate source and the EKF was enabled. Figure 9 shows the attitude control errors during the longest operation to date. At the beginning of the span there are two small slews in pitch and yaw, and at the end of the span there is a 30 deg roll slew. Figure 9 shows that the gyroless EKF is, for the most part, meeting the original gyro-based attitude control requirement. The spikes outside the requirement (other than the slews) occur during zero wheel speed crossings and are likely linked to mis-modeled drag in the reaction wheels. Figure 10 shows the complementary filter rate estimate during the 30 deg roll slew. Figure 11 is the EKF estimated bias. There is a clear orbital rate component in the estimated bias. The

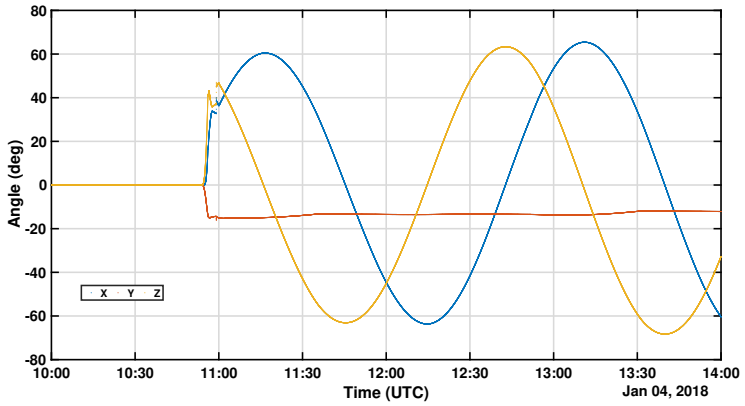

Figure 7. Large EKF Attitude Error Angles (Truth Compared to Estimated) During a Prolonged Simultaneous Star Tracker Occultation

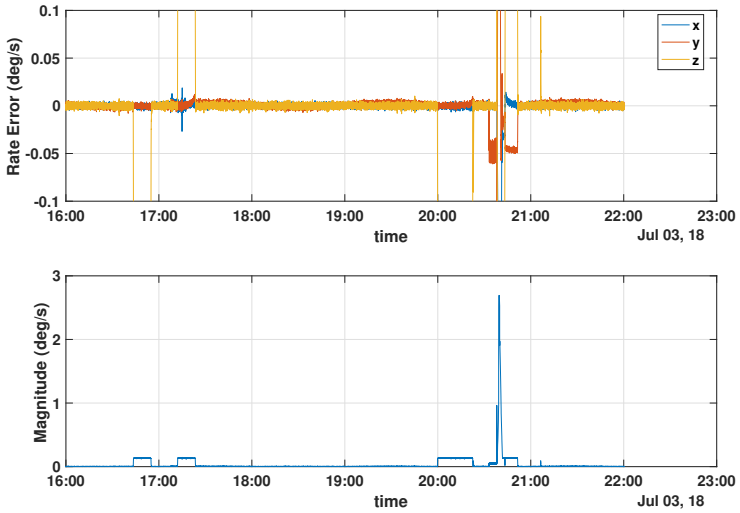

Figure 8. FlatSat Test. Controller Rate Errors During Yaw Slews and Stationkeeping Maneuver

EKF will continue to be analyzed and tuned to optimize performance. Analysis is also underway to determine if updating the onboard reaction wheel friction coefficients will improve the ACS performance during low wheel speeds.

CONCLUSIONS AND FUTURE WORK

LRO has been making remarkable discoveries contributing to the understanding of the moon for over nine years. The MIMU was powered off in March 2018 following a decline in the laser intensity monitor current. The spacecraft continued to observe the moon, but only in a nadir pointing mode, relying on star tracker derived rates. Slews to science targets of interest were suspended. A complementary filter was developed that combines low frequency star tracker differentiated quaternions with high frequency integrated accelerations from the reaction wheel control torques. The complementary filter rate replaces the gyro rate in the extended Kalman filter, resulting in minimal flight software changes. The new rate estimate was incorporated first into a high-fidelity simulation

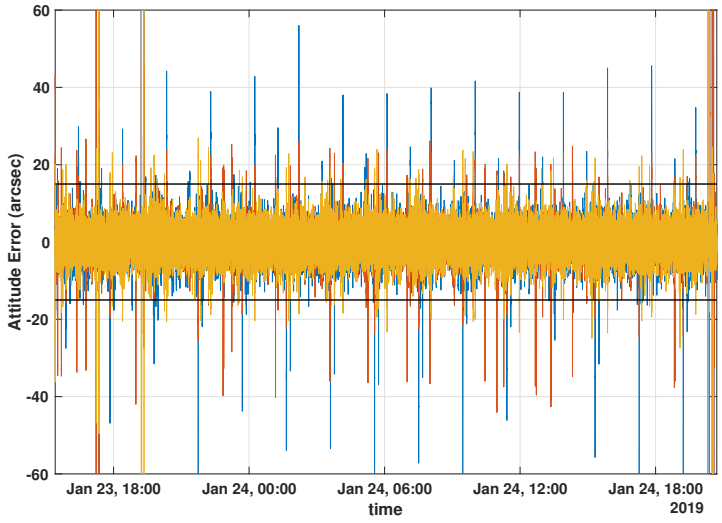

Figure 9. Inflight Test, Controller Attitude Errors (X = Blue, Y = Red, Z = Yellow), With Gyro-Based Attitude Control Requirement (Black Line)

and then developed into flight code. Extensive ground testing was performed simulating a variety of operational scenarios. The revised flight software was uploaded to the spacecraft in December 2018. The estimation and control errors showed considerable improvement, and the spacecraft has successfully slewed several times. Inflight testing will continue in order to optimize performance. After the inflight testing is concluded LRO will return to nominal science operations, once again collecting detailed observations of the moon.

ACKNOWLEDGMENT

The authors would like to thank the LRO Flight Operations Team for their excellent support of the LRO mission and their help in successfully delivering the new software to the spacecraft.

REFERENCES

[1] "Lunar Reconnaissance Orbiter," website. https://lro.gsfc.nasa.gov.

[2] P. C. Calhoun and J. C. Garrick, "Observing Mode Attitude Controller for the Lunar Reconnaissance Orbiter," NASA Technical Reports Server, March 2008. https://ntrs.nasa.gov.

[3] P. Calhoun, "MIMU Failure Risk Mitigation Trade Study, ST Derived Rates for Use in LRO Observing Mode," Presentation, August 2014. Internal NASA Goddard Space Flight Center document.

[4] F. L. Markley and J. L. Crassidis, *Fundamentals of Spacecraft Attitude Determination and Control*. Springer, 2014.

[5] S. Park and J. How, "16.333: Lecture 15, Inertial Sensors, Complementary filtering, Simple Kalman Filtering," Presentation, 2004. https://ocw.mit.edu/courses/aeronautics-and-astronautics/16-333-aircraft-stability-and-control-fall-2004/lecture-notes.

[6] J. W. Murrell, "Precision Attitude Determination for Multimission Spacecraft," *AIAA Guidance and Control Conference*, Palo Alto, California, August 1978.

[7] J. Edward Falkenhayn, "Mutlimission Modular Spacecraft (MMS)," *AIAA Space Programs and Technologies Conference*, Houston, Texas, June 1988.

[8] J. Halverson, R. Harman, R. Carpenter, and D. Poland, "Tuning the Solar Dynamics Observatory Onboard Kalman Filter," *AIAA/AAS Astrodynamics Specialist Conference*, No. AAS 17-591, Stevenson, Washington, August 2017.

[9] M. Wright, "Lunar Reconnaissance Orbiter FlatSat," NASA Technical Reports Server, October 2008. https://ntrs.nasa.gov.

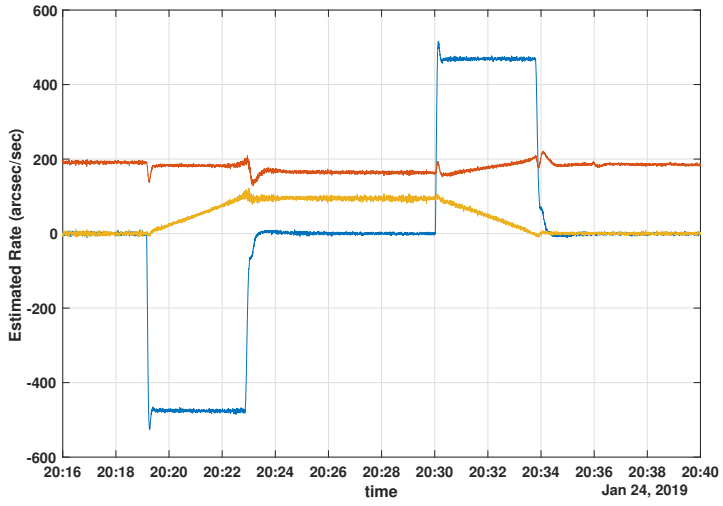

Figure 10. Inflight Test, 30 Deg Roll Slew (X = Blue, Y = Red, Z = Yellow)

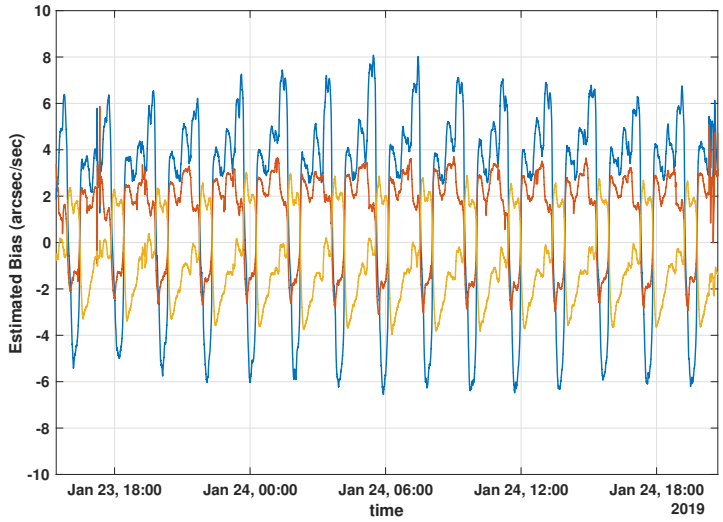

Figure 11. Inflight Test, Bias Estimate (X = Blue, Y = Red, Z = Yellow)